Groundwater Monitoring&Remediation

Seasonal to Decadal Variability in Focused Groundwater and Contaminant Discharge along a Channelized Stream

by Ganesh N. Tripathi, Alan E. Fryar, Steven K. Hampson, Abhijit Mukherjee

AQ1

Abstract

Focused groundwater discharge to streams is problematic at contaminated sites because high fluxes can limit natural attenuation in the hyporheic zone. However, information on location, spatial evolution, and temporal persistence of springs in unlithified sediments over multiyear time scales is limited. We examine discharge at point (~1-m) to reach (~300-m) scales along a stream that intercepts trichloroethene and technetium-99 plumes from a Superfund site. During 2011 to 2012, we seasonally monitored stream and spring flow and contaminant concentrations, along with probing streambed temperatures on a grid in winter and summer, building on prior monitoring during 1999 to 2002. Baseflow measured by both gauging and dye dilution generally increased with distance downstream, and stream and spring discharge varied seasonally, from minima in October to January to maxima in February to June. Thermal anomalies identified by probing occupied approximately 3% to 6% of the reach and typically coincided with visible springs or seeps. Locations of anomalies were similar to those identified in summer 2002, although some orifices disappeared and others emerged. Vertical groundwater fluxes calculated from probing tended to be less than net fluxes calculated from stream discharge, perhaps in part because the assumption of one-dimensional, steady-state flow in calculating point fluxes was simplistic. Maximum contaminant concentrations and fluxes decreased between 1999 to 2001 and 2011 to 2012 as a result of partial capture by an upgradient pump-and-treat system. Our findings confirm that springs in unlithified sediments can remain stationary within a few meters over decadal time scales, and seasonal variability in discharge can be greater than decadal variability.

Introduction

Groundwater discharge can be focused where stratigraphic heterogeneities and discontinuities (e.g., joints, fractures, and soil pipes) occur within or beneath streambed or bank sediments. For example, "sand boils" can form when upward flow suspends sand-sized clasts (Guhman and Pederson 1992). Focused discharge of contaminated groundwater is problematic because relatively high fluxes can limit natural attenuation by sorption and biodegradation in the hyporheic zone (LaSage et al. 2008a; Weatherill et al. 2014, 2018). A combination of techniques covering a range of spatial scales, from submeter (at springs and seeps) to hundreds of meters (along stream reaches), can differentiate focused from diffuse discharge (Hyun et al. 2011; Kikuchi et al. 2012; Krause et al. 2012; Briggs et al. 2013; Hare et al. 2015; Poulsen et al. 2015; Rosenberry et al. 2016; Stelzer et al. 2017). Physical techniques include seepage meters, sequential streamflow gauging using a current meter, and hydraulic-gradient measurements using streambed piezometers or a potentiomanometer. Chemical techniques include measurement of ambient or introduced solute tracers (including contaminants) along gaining reaches. Thermal techniques, which rely on temperature contrasts between groundwater and streams, include temperature probing, installing vertical arrays of thermistors in the streambed, thermal infrared cameras, and fiber-optic distributed temperature sensing. In particular, temperature probing is a relatively simple, rapid method for delineating sites of groundwater inflow (White et al. 1987; Fryar et al. 2000; LaSage et al. 2008b) and for calculating vertical (upward) groundwater discharge fluxes (Conant 2004; Schmidt et al. 2006, 2007).

Information on the spatial evolution and temporal persistence of springs in unlithified sediments is limited. Erosion during focused discharge (piping) occurs as positive pore pressures create shear and tension stresses (Hagerty 1991a, 1991b; National Research Council 2004), causing bank and bed failure. The dynamic nature of piping, coupled with fluvial deposition and erosion, suggests that discharge points should evolve spatially over some time scale. Sand boils can be ephemeral features associated with flooding, when elevated river stages result in heightened hydraulic gradients beyond levees (Li et al. 1996; Davidson et al. 2013), and with earthquake-induced liquefaction (Lin et al. 2003). However, sand boils can also be perennial at time scales as long as a century (Guhman and Pederson 1992).

Article impact statement: Springs in unlithified sediments can remain relatively stationary and maintain relatively uniform ranges of discharge over a decade.

doi: 10.1111/gwmr.12422

There is a lack of published studies on variability in focused discharge of contaminated groundwater in unlithified sediments over multiyear time scales. Building on previous monitoring, we address focused discharge along a first-order perennial stream in the Gulf Coastal Plain of Western Kentucky (United States). At this site, springs have been observed since at least 1989 (Evaldi and McClain 1989) and dissolved trichloroethene (TCE) was first observed in springs in 1998 (Fryar et al. 2000). Groundwater discharge and contaminant fluxes were concentrated along a channelized reach and varied seasonally, with natural attenuation of TCE being dominated by volatilization (LaSage et al. 2008a, 2008b). Using seasonal monitoring of stream and spring flow and contaminant concentrations, along with streambed temperature probing in winter and summer, we examine variability in fluxes of groundwater and contaminants at spatial scales of meters to hundreds of meters and at seasonal to decadal time scales. We discuss constraints on monitoring focused discharge and the effects of remediation on contaminant fluxes.

Study Area Background

The Little Bayou Creek watershed occupies 25 km^2 in McCracken County, Kentucky (Figure 1a. Surface elevation ranges from 116 m above sea level (asl) to 88.4 m asl at the Ohio River (pre-2018 pool elevation). Land use in the basin includes industry (the U.S. Department of Energy [DOE] Paducah Gaseous Diffusion Plant [PGDP], which enriched uranium from 1952 to 2013, and the Tennessee Valley

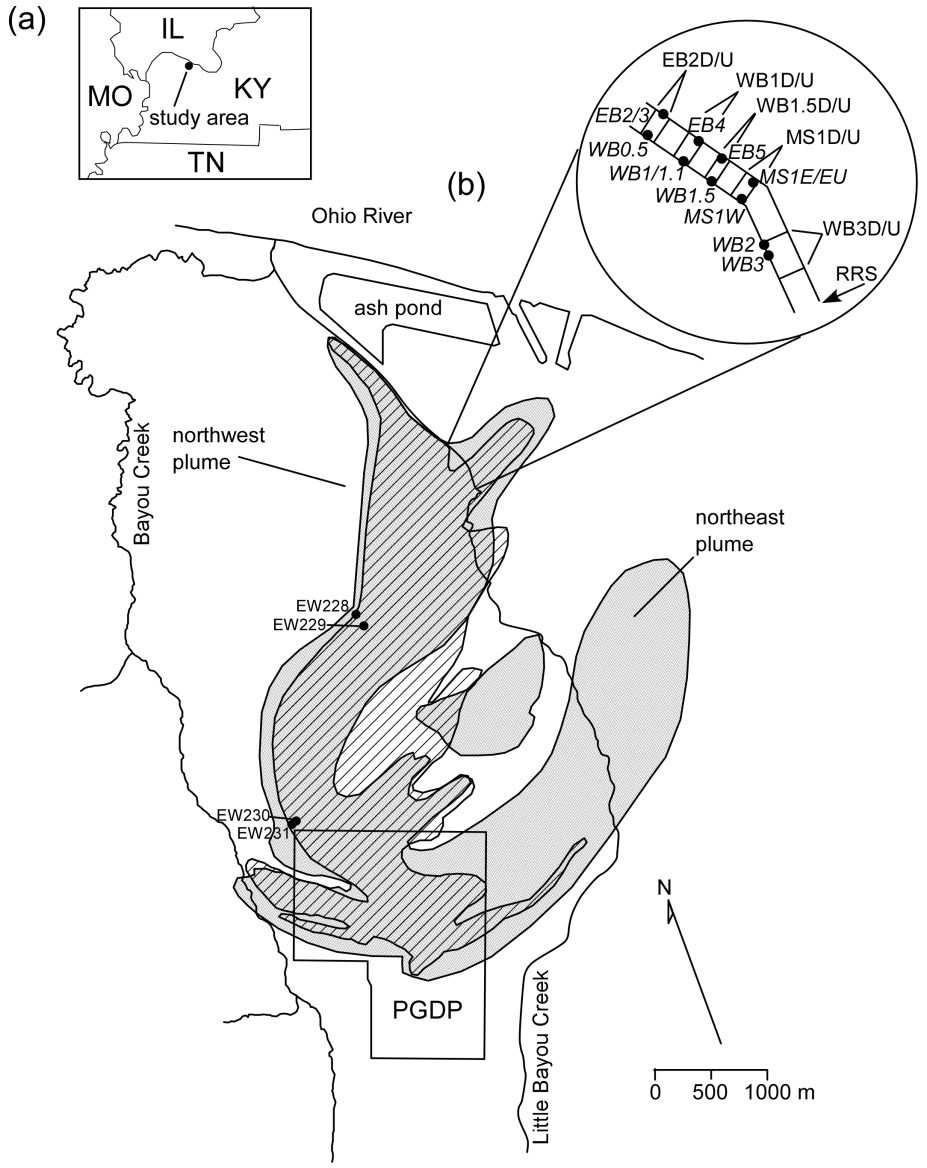

Figure 1. (a) Regional location of study area. KY = Kentucky, IL = Illinois, MO = Missouri, TN = Tennessee. PGDP is located at latitude 37°06′N, longitude 88°48′W. (b) Study-area map with groundwater contaminant plumes circa 2010. Inset (not to scale) shows stream-monitoring sites (D and U suffixes and RRS) and springs (in italics). Stippled areas indicate TCE concentrations ≥5 µg/L; hachured areas indicate ^{99}Tc concentrations ≥25 pCi/L. EW refers to extraction well. Modified from Journal of Hydrology, vol. 360, LaSage, D.M., A.E. Fryar, A. Mukherjee, N.C. Sturchio, and L. Heraty, Groundwater-derived contaminant fluxes along a channelized Coastal Plain stream, 265 to 280, Copyright 2008, with permission from Elsevier.

Authority [TVA] Shawnee Fossil Plant, a coal-fired generating station), the West Kentucky Wildlife Management Area (interspersed woodlands and fields), and rural residences and farms. Little Bayou Creek (11 km long) was a tributary to the Ohio River prior to industrialization. Between 1953 and 1971, the lower 2.5-km reach was channelized around ash ponds at the Shawnee Plant and connected to Bayou Creek 340 m southwest of the river. Discharge of process water from PGDP near the creek's headwaters maintained baseflow. In the river's floodplain, Little Bayou Creek is a type F5 stream (Rosgen and Silvey 1998), marked by entrenchment (~2 to 5 m below the surrounding landscape), meanders, riffle-pool morphology, high width/depth ratio, and low gradient (LaSage et al. 2008b).

The regional climate is humid-warm temperate (Köppen classification Cfa; Bruegger 2017). At the Paducah station of the National Weather Service (NWS), 6 km southeast of PGDP, annual precipitation averaged 1.25 m during 1981 to 2010, with average monthly rainfall ranging from 70 mm in August to 125 mm in May (University of Kentucky Agricultural Weather Center 2020b). Monthly air temperatures were lowest in January (daily average range −3.3 to 6.1 °C) and highest in July (daily average range 20.6 to 31.7 °C). During this study (January 1, 2011 to February 29, 2012), maximum 1-d precipitation occurred April 24, 2011 (103 mm; University of Kentucky Agricultural Weather Center 2020a). Precipitation for calendar year 2011 totaled 1.92 m. Daily air temperatures ranged from −20.0 °C on February 10, 2011, to 37.2 °C on three dates in August and September 2011.

The watershed is underlain by Mississippian limestone at approximately 91 to 122 m below land surface (bls). Bedrock is overlain by the Upper Cretaceous McNairy Formation, which consists of fluvial-deltaic sands, silts and clays (Clausen et al. 1992). The McNairy Formation is successively overlain by the Paleocene Porters Creek Clay, Miocene-Pleistocene continental deposits (fining upward from cobbles and gravel), Pleistocene loess and Holocene alluvium (Olive 1980; Clausen et al. 1992). The lower and upper continental deposits are equivalent to the Mounds Gravel and the Metropolis Formation, respectively, of southern Illinois (LaSage et al. 2008b). In the vicinity of PGDP, the Mounds Gravel has been informally termed the regional gravel aquifer (RGA) (Clausen et al. 1992).

In general, groundwater flows in the RGA north-northeast toward the Ohio River, although hydraulic gradient reversals occur when the river is at flood stage (Clausen et al. 1992; Fryar et al. 2000). The direction of flow appears to be controlled in part by northeast-southwest trending faults (Almayahi and Woolery 2018). Flow is predominantly vertical in the overlying semi-confining unit (Metropolis Formation). The aquifer is recharged by precipitation and, historically, by leakage from lagoons and water mains at PGDP (LaSage et al. 2008b). Diffuse groundwater discharge occurs where the creeks are incised into the RGA and alluvium in the Ohio River floodplain (Fryar et al. 2000; LaSage et al. 2008b). In addition, springs are visible in the banks and bed along the upper approximately 300 m of the channelized segment of Little Bayou Creek, where sand locally mantles hard, mottled clay. The springs appear to coincide with meter-scale heterogeneities in the Metropolis Formation, such as sand stringers or fractures, which may have been enhanced by channelization (LaSage et al. 2008b).

Groundwater in the RGA is contaminated by TCE, which was used as a degreasing solvent at PGDP from 1953 to 1993, and by technetium-99 (^{99}Tc), a radionuclide that was a byproduct of reprocessed uranium oxide use from 1953 to 1976 (Clausen et al. 1992; LaSage et al. 2008a). The Safe Drinking Water Act sets a maximum contaminant level (MCL) of 5 µg/L for TCE, while ^{99}Tc (a beta emitter with a half-life of 2.1×10^5 year) has a site-derived MCL of 900 pCi/L. Offsite groundwater contamination was first detected in 1988 and PGDP was added to the National Priorities List (Superfund) in 1994. Two primary contaminant plumes (northwest and northeast) extend several kilometers from PGDP toward the Ohio River (Figure 1b). Concentrations in the suspected source areas approached the solubility limit for TCE (1100 mg/L, which is indicative of residual amounts of dense, nonaqueous phase liquid) and 40,000 pCi/L for ^{99}Tc. LaSage et al. (2008a) reported maximum concentrations of 450 µg/L for TCE and 461 pCi/L for ^{99}Tc in springs, and a maximum TCE concentration of 1691 µg/L in a peeper (passive-diffusion sampler) beneath the streambed, where the northwest plume passes beneath Little Bayou Creek. There is no evidence that the northeast plume impacts water quality in Little Bayou Creek (LaSage et al. 2008a). Pump-and-treat systems were implemented for contaminant removal in the northwest plume in August 1995 (U.S. Department of Energy 2007).

Methods

Stream and Spring Gauging

Stream flow was gauged by wading with a current meter and top-setting rods (Marsh-McBirney, Frederick, Maryland) on January 23, June 23, and October 22, 2011, and February 19, 2012. Gauging occurred when no precipitation had been recorded for at least 24 h at the Paducah NWS station. In contrast to LaSage et al. (2008b), who gauged at only two locations along the reach, we gauged along five pairs of transects downstream and upstream of visible springs (sites with D and U suffixes, respectively; Figure 1b). Velocity and stream depth were typically measured at 6-inch (0.15-m) to 1-foot (0.30-m) intervals. Stream discharge Q_g was calculated using the midsection method of Rantz (1982).

We also measured stream discharge by dilution of a 5% rhodamine WT (RWT) dye solution on January 22, June 24, and October 24, 2011, and on February 20, 2012. Following Mukherjee et al. (2005), we added 150 mL of RWT solution to each of two carboys containing 20 L of stream water, manually mixed them, and poured them in a single injection across the width of the stream at the upstream end of the study reach. Samples were collected at four downstream locations (WB3U, MS1U, WB1.5D, and EB2D) (Figure 1b). At each site, the first grab sample was collected midstream in a 40-mL amber glass vial prior to arrival of the visible dye cloud. Samples were collected at approximately the same location when the cloud arrived and at intervals of 2 to 10 min thereafter, depending on distance from the injection point and time since injection, until the cloud passed.

During each tracer test at each monitoring location, 18 to 29 samples were collected for a duration of 143 to 240 min following dye arrival. After each tracer test, samples were refrigerated (for 1 to 3 weeks) until approximately 24 h prior to analysis. Samples were analyzed at the Kentucky Geological Survey (KGS) on a Varian Cary Eclipse fluorescence spectrophotometer (Agilent Technologies, Santa Clara, California). Stream discharge (Q_{dye}) was calculated for each sampling location following Kilpatrick and Cobb (1985):

$$Q_{dye} = 5.89 \times 10^{-7} \left(\frac{S_G V_S C_S}{A_C} \right) \quad (1)$$

where S_G is the specific gravity of the dye solution (1.03), V_S is the volume of concentrated dye solution, C_S is the concentration of injected dye, and A_C is the area under the breakthrough curve.

Discharge for selected bank springs (Q_{spr}) was recorded on January 24, June 23, and October 22, 2011, and on February 18, 2012. We measured Q_{spr} where the orifice was located above stream stage and flow could be captured in a bucket or other container. We used a stopwatch to measure the duration of flow and a graduated cylinder to measure volume. We repeated this process twice for each monitoring event at each spring and calculated the average discharge, except for springs MS1E and WB3 in February 2012, when a cut-throat flume (Baski, Denver, Colorado) was used. The coefficient of variation was ≤21% for the 18 sets of triplicate discharge measurements and was ≤11% for 16 of those sets.

Temperature Probing

Streambed temperature was measured on a grid using a 1.24-m-long, 6-mm-diameter, stainless-steel probe connected to a digital thermometer (YSI, Yellow Springs, Ohio). Probing occurred along transects at intervals of 10 feet (3 m) along the stream and 3 feet (0.9 m) across it. At each point, temperature was recorded to the nearest 0.1 °C at the sediment-water interface and the maximum (refusal) depth to which the probe could be pushed manually (LaSage et al. 2008b). This allowed delineation of streambed topography beneath mobile bed sediment. Measurements were made along the 307 to 308 m reach on January 4 to 8, 2011 (823 points), and August 5 to 9, 2011 (683 points). Different numbers of points for each set of measurements reflect seasonal differences in stream width (probing did not extend beyond the wetted perimeter). Because of bends, the reach was divided into segments, and temperature was mapped along each using natural neighbor interpolation in Surfer 9 (Golden Software, Golden, Colorado).

Sampling and Field Parameter Measurements

Groundwater and surface-water samples were collected during each round of field work (January 2011, June 2011, October 2011 and February 2012). Samples were collected simultaneously with stream gauging in June and February. Surface-water sampling was done before dye tracing on January 22. Groundwater (spring) sampling was done on January 24 along with field parameter measurements and spring discharge measurements. Most samples were collected during gauging on October 22, but some samples were collected the following day. Samples for TCE and other volatile organic compounds (VOCs) were collected in 40-mL amber glass vials with Teflon-lined screw caps, with exclusion of headspace and addition of 4 to 5 drops of 6 N HCl as a preservative. Technetium-99 samples were collected in 1-L high-density polyethylene (HDPE) bottles following the same procedure as for VOC samples, but without preservatives. VOC samples were refrigerated and submitted within 1 week for analysis by USEPA method 8260B (gas chromatography-mass spectrometry) at McCoy and McCoy Laboratories (Madisonville, Kentucky). Technetium-99 samples were analyzed by liquid scintillation counting in September 2012 at Eberline Services (Oak Ridge, Tennessee).

We measured groundwater and surface water temperatures using a YSI multifunction meter at gauging locations and selected springs in January, June, and October 2011 and February 2012. Dissolved oxygen (DO) was measured by Winkler titration (Wood 1976) using a Hach kit (Hach Company, Loveland, Colorado) for springs in June 2011, October 2011, and February 2012.

Results

Stream and Spring Discharge

Gauged discharge did not increase monotonically downstream along the study reach (Figure 2), but occasional decreases in Q_g between successive sites were within measurement error (−40.3% to +29.2%; within ±30% for 38 of 40 runs). Values of Q_g always increased along segments in the vicinity of springs at the upstream (WB3D-WB3U) and downstream (EB2D-EB2U) ends of the reach. Gauged discharge was always greater at the farthest downstream site (EB2D) than at the farthest upstream site (WB3U), indicating the reach was gaining overall. Increases in Q_g along the reach (ΔQ_g) ranged from 9.1 L/s in January 2011 to 44.2 L/s in February 2012. Except for WB1.5D and EB2D in January 2011, discharge computed from dye dilution continuously increased downstream (Figure 2). Values of Q_{dye} at both ends of the reach were lowest in January 2011 (15.7 L/s at WB3U and 28.3 L/s at EB2D) and highest in February 2012 (35.1 L/s at WB3U and 68.5 L/s at EB2D). Increases in Q_{dye} along the reach (ΔQ_{dye}) ranged from 12.7 L/s in January 2011 to 34.5 L/s in June 2011.

Net stream fluxes between pairs of gauging sites or dye-monitoring sites were estimated as:

$$q_{net} = \left(Q_d - Q_u\right) / \left(w_{avg} \times l\right) \quad (2)$$

where Q_d and Q_u are discharge (measured by gauging or dye dilution) at the up- and downstream ends of the stream segment, w_{avg} is the average width of the segment (measured by gauging), and l is its length. Values of q_{net} were positive in 24 of 36 instances for gauging and in 11 of 12 instances for dye dilution (Table S1, Supporting Information). Positive values ranged from 2.52×10^{-6} to 5.59×10^{-4} m/s (median 3.29×10^{-5} m/s) for gauging and from 2.15×10^{-6} to 5.86×10^{-5} m/s (median 1.66×10^{-5} m/s) for dye dilution. Considering the same subreaches (MS1U-WB3U, WB1.5D-MS1U, and EB2D-WB1.5D) as measured for dye dilu-

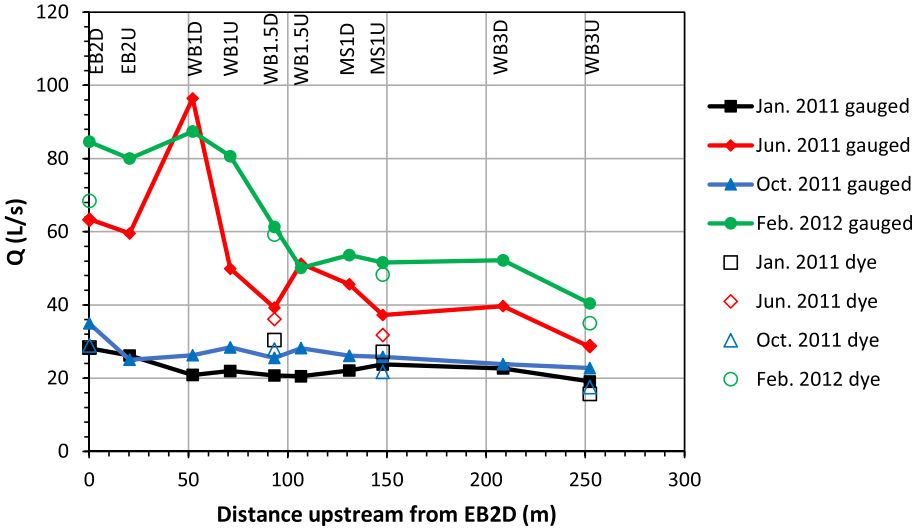

Figure 2. Stream discharge Q measured by gauging and dye dilution at different sites along the study reach for January 2011, June 2011, October 2011, and February 2012.

Table 1

Discharge, Temperature and DO Concentrations for Monitored Springs

	January 2011		June 2011			October 2011			February 2012		
	Q_{spr} (L/s)	T (°C)	Q_{spr} (L/s)	T (°C)	DO (mg/L)	Q_{spr} (L/s)	T (°C)	DO (mg/L)	Q_{spr} (L/s)	T (°C)	DO (mg/L)
WB3	0.271	13.5	2.10	14.0	2.96	0.590	15.3	2.98	2.14	14.3	3.32
WB2	0.0064	10.1	0.179	13.9	3.76	0.0252	15.0	3.74	0.139	14.1	3.64
MS1W		12.0		14.2	2.96		14.8	2.60		14.1	3.10
MS1EU							14.6	3.74		14.4	3.90
MS1E			1.69	14.1	3.60		14.6	3.62	0.411	14.2	4.18
EB5	0.0108	9.4	0.198	13.9	4.18	0.0364	15.0	2.84	0.113	13.3	3.62
WB1	0.100	12.0	0.274	14.0	3.28	0.107	15.2	3.36	0.308	13.3	3.92
EB4						0.214	14.9	3.34		10.8	
EB3				14.0	3.84					13.3	4.50
WB0.5				14.1	3.90						
EB2	0.0525	13.3		13.8	3.90		15.2	3.62		14.1	3.78

Discharge values represent averages of triplicate measurements using graduated cylinder and stopwatch except for WB3 and MS1E for February 2012 (cut-throat flume used). Blank indicates no measurement.

tion, 10 of 12 q_{net} values for gauging were positive (range 4.91×10^{-6} to 5.21×10^{-5} m/s; median 1.72×10^{-5} m/s).

Measured spring-discharge values ranged from 0.0064 to 2.14 L/s (Table 1) and were always greatest at WB3 (the farthest upstream spring). WB3 was one of four springs with flow measurements during each monitoring round; of these, WB1 always had the second largest value, followed by EB5 and WB2. Values of Q_{spr} were lowest in January 2011 and highest in June 2011 or February 2012. Flow was monitored when feasible at three other springs (MS1E, EB4, and EB2). For the stream segment WB3D-WB3U, the combined Q_{spr} from WB3 and WB2 represented 5.0% to 21% of the gauged increase in discharge. When flow could be measured at MS1E (June 2011 and February 2012), Q_{spr} represented 20% of the gauged increase in discharge along the stream segment MS1D-MS1U. The contribution of Q_{spr} to gauged stream discharge for segments farther downstream was <5.0% or could not be determined. The total contribution of Q_{spr} for all springs to the gauged increase in discharge along the study reach (ΔQ_g) ranged from 4.8% in January 2011 to 13% in June 2011.

Spring, Stream, and Streambed Temperatures

Temperatures for monitored springs varied from 9.4 to 13.5 °C (median 12.0 °C) in January 2011 to 14.6-15.3 °C (median 15.0 °C) in October 2011 (Table 1). Stream temperatures varied from 0.66 to 2.05 °C (median 1.37 °C) in January 2011 to 22.5-25.8 °C (median 23.4 °C) in June 2011.

Penetration depth for the temperature probe was controlled by the occurrence of the Metropolis Formation beneath bed sediment. The depth at which temperature was measured varied from 0.01 m to the entire probe length (1.24 m). Broadly speaking, temperature increased with depth in January 2011 and decreased with depth in August

2011, converging toward 14 °C (Figure 3). However, at focused discharge points, measured temperature was several degrees higher than median stream temperature in January and lower than median stream temperature in August, even at shallow depth.

In January 2011, temperatures measured by probing were 0.6 to 14.5 °C (median 3.6 °C) at the sediment-water interface and 1.3 to 14.0 °C (median 5.1 °C) at refusal depth. Interpolated temperature maps show anomalies (warmer) at the interface and at depth (Figure 4). Along reach (segment) 1, anomalies associated with springs WB3 and WB2 were evident at approximately 225 and 215 m, respectively. Another anomaly at approximately 190 m did not coincide with a visible spring. Along reach 2, the west-bank anomaly at approximately 145 m coincided with spring MS1W and the east-bank anomaly at approximately 140 m with spring MS1E. The midstream anomaly on the refusal-depth map between approximately 110 and 115 m was not evident on the interface map, but appeared to coincide with soft sediment observed along the east bank near 110 m. Anomalies on the refusal-depth map between approximately 95 and 100 m coincided with west-bank spring WB1.5 and east-bank spring EB5; a nearby midstream anomaly was not visible in the field. Along reach 3, a broad anomaly for the segment between approximately 5 and 30 m, which coincided with spring EB2, appeared to be dominated by groundwater discharge.

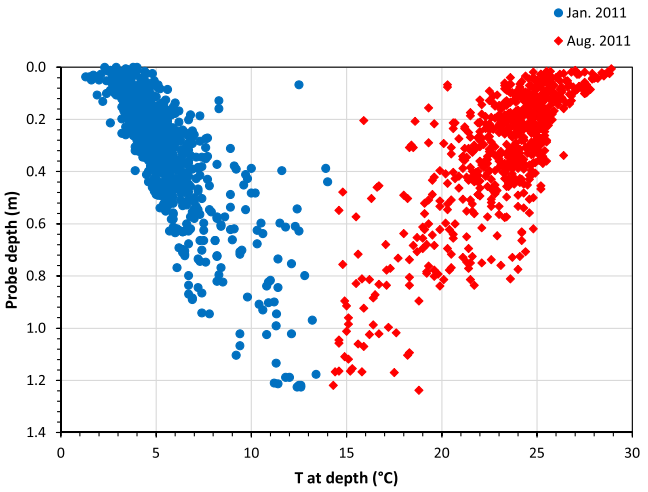

Figure 3. Probe refusal depth versus temperature at depth for January 2011 and August 2011.

In August 2011, probed temperatures were 14.6 to 29.1 °C (median 25.4 °C) at the sediment-water interface and 14.3 to 28.9 °C (median 23.8 °C) at refusal depth. Anomalies (cool) tended to coincide with anomalies (warm) observed in January (Figure 4). Along reach 1, anomalies persisted close to springs WB2 and WB3 at approximately 215 to 225 m and emerged approximately 15 m upstream of WB3 on both interface and refusal-depth maps. The anomaly at approximately 190 m near the west bank appears only on the refusal-depth map. Along reach 2, anomalies were again associated with springs MS1W (~145 m), MS1E (~140 m), and EB5 (~97 m). Along reach 3, anomalies coin-

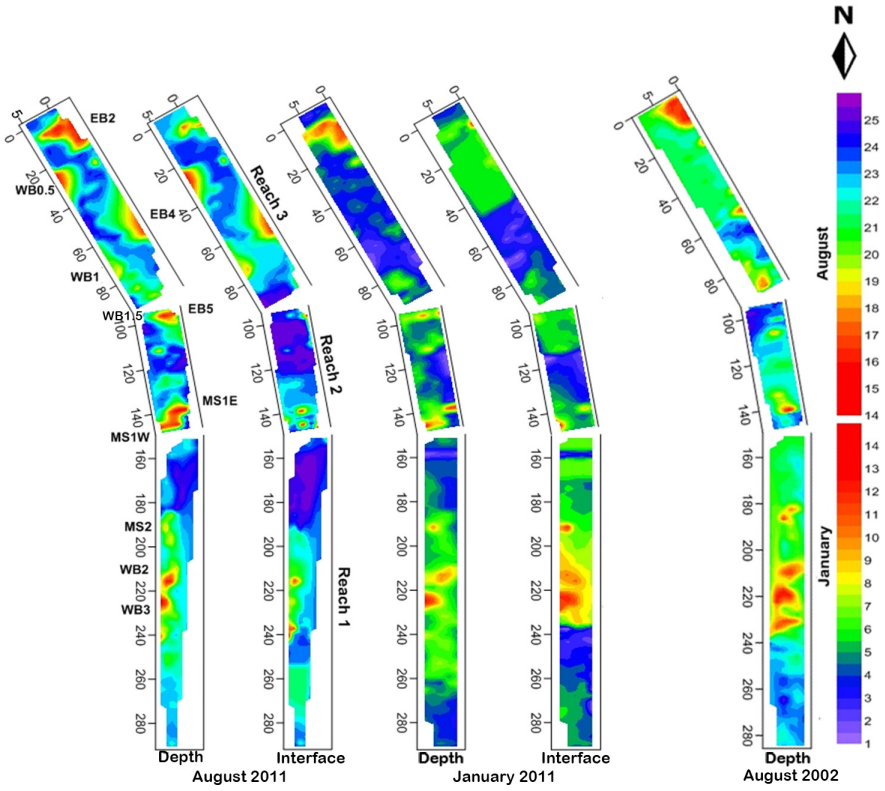

Figure 4. Temperature distribution (in °C) at probe refusal depth and at the stream-sediment interface for January 2011 and August 2011 and at probe refusal depth for August 2002 (after LaSage et al. 2008b). Distances across and along stream are in m. Note that true orientation of reach 2 is same as reach 3 (N30°W).

cident with springs WB1 (~75 m), EB4 (~60-65 m), WB0.5 (~25 m), and EB2 (~5 m) appear on both maps.

We calculated the groundwater discharge flux at each probing site, assuming one-dimensional (1D, vertical) and steady-state conditions (Turcotte and Schubert 1982; Schmidt et al. 2007):

$$q_z = -\frac{K_{fs}}{\rho_f c_f z} \ln \frac{T(z) - T_L}{T_0 - T_L} \quad (3)$$

Here K_{fs} is the saturated thermal conductivity, ρ_f c_f is the volumetric heat capacity of water (4.19×10^6 J/[m^3-K]), $T(z)$ is temperature measured at depth z, T_0 is stream temperature, and T_L is groundwater temperature. We assumed a value of 2.0 J/(s-m-K) for K_{fs} (Schmidt et al. 2007), took T_L = 14 °C, and, following Schmidt et al. (2007), took T_0 as the mean at the sediment-water interface for each 5-d run (3.7 °C in January, 25.5 °C in August). Positive values of q_z were obtained for 712 points (86.5%) in January and for 582 points (85.2%) in August. Physically nonsensical values resulted for $T(z) \le T_0$ or $\ge T_L$ in January and for $T(z) \ge T_0$ in August. Positive q_z values ranged from 7.7×10^{-9} to 1.4×10^{-5} m/s (median 2.8×10^{-7} m/s) for January and from 6.5×10^{-9} to 4.3×10^{-6} m/s (median 3.6×10^{-7} m/s) for August. The lowest q_z values ($<4 \times 10^{-8}$ m/s) resulted as $T(z)$ approached T_0 (Figure 5), which occurred for $z \le 0.5$ m. However, the highest q_z value also occurred at relatively shallow depth (0.067 m).

Stream and Spring Chemistry

Contaminant concentrations in stream water ranged from below method detection limit (BDL; <5 µg/L) to 120 µg/L for TCE and from BDL (<4.3-4.8 pCi/L) to 72.74 pCi/L for ^{99}Tc (Table 2). Highest concentrations of both TCE and ^{99}Tc were measured in October 2011 for the east-bank tributary RRS, upstream of WB3U, which was sampled during the final two rounds. At other sites, maximum concentrations occurred in June (TCE 20-28 µg/L, ^{99}Tc 11.81-18.67 pCi/L) and minimum concentrations occurred in January (TCE BDL-8.4 µg/L, ^{99}Tc 1.65-4.98 pCi/L). Concentrations of TCE and ^{99}Tc in stream water tended to track each other when stream discharge was elevated in June 2011 and February 2012 (Figure 6).

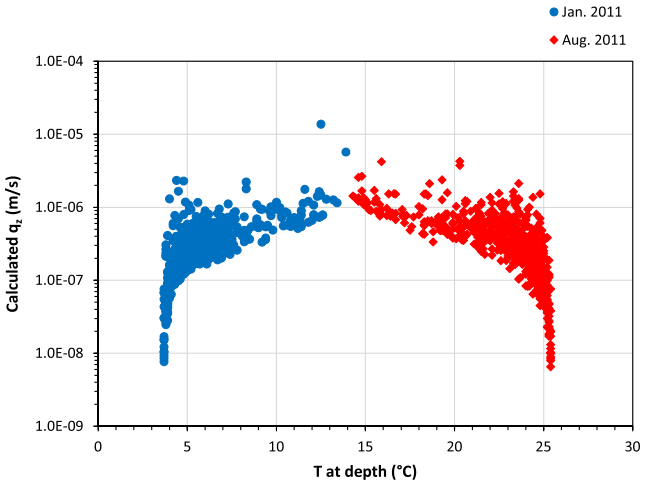

Figure 5. Upward groundwater flux calculated from temperature probing (q_z) versus temperature at depth. Values of $q_z \le 0$ are omitted.

Contaminant concentrations in groundwater ranged from BDL to 160 µg/L for TCE and from BDL to 51.68 pCi/L for ^{99}Tc (Table 3). Concentrations were highest at WB3 in January 2011 and were lowest (BDL for all sampling rounds) at EB2. For each of the four springs where both TCE and ^{99}Tc were always detected (WB1, MS1W, WB2, and WB3), concentrations varied by a factor of less than 3 and did not show consistent seasonal variations. In general, TCE and ^{99}Tc concentrations decreased asymptotically from upstream to downstream springs for all sampling rounds and were lower for east- than west-bank springs. However, TCE and ^{99}Tc were higher for the east-bank spring MS1EU than for the upstream west-bank spring WB2 in October 2011 and were higher for MS1EU than for both WB2 and WB3 in February 2012. Considering the entire groundwater dataset, a strong linear relationship between the contaminants is evident (Figure 7). Groundwater DO fell within a relatively narrow range (2.60-4.50 mg/L) and, for eight of nine springs with multiple measurements, varied by <1 mg/L between sampling rounds (Table 1).

Contaminant fluxes were calculated for individual springs at different times as

$$F_{spr} = C \times Q_{spr} \quad (4)$$

where C is the TCE or ^{99}Tc concentration. For each sampling round and contaminant, F_{spr} was greatest at WB3 (43-210 µg/s for TCE and 14-79 pCi/s for ^{99}Tc; Table S2, Supporting Information). Maximum F_{spr} values occurred in February 2012 for TCE and in June 2011 for ^{99}Tc. Reach-scale contaminant fluxes were calculated as

$$F_r = C_d Q_d - C_u Q_u \quad (5)$$

where d and u represent EB2D and WB3U, respectively. For each contaminant, F_r values determined by gauging and dye dilution were relatively similar: 150 to 860 µg/s for gauging and 150 to 820 µg/s for dye dilution for TCE; 77 to 310 pCi/s for gauging and 89 to 310 pCi/s for dye dilution for ^{99}Tc (Table S2, Supporting Information). Values of F_r were highest in June 2011 except for the TCE flux from gauging, which was highest in February 2012. The relatively small differences in contaminant concentrations in stream water between WB3U and EB2D magnify the effects of measurement uncertainty on F_r calculations.

Discussion

Comparison of Stream Discharge and Groundwater Flux Values

Discharge values from gauging, dye dilution, and individual springs, as well as the predominance of positive (upward) flux values calculated from temperature probing, corroborate prior observations that the study reach is gaining. Decreases in Q_g between successive gauging transects, while within the calculated error range, may

Table 2

TCE and ^{99}Tc Concentrations in Stream Water

	January 2011		June 2011		October 2011		February 2012	
RRS								
TCE (µg/L)					120		29	
^{99}Tc (pCi/L)					72.74	±8.20	8.54	±3.08
WB3U								
TCE (µg/L)	<5		20		<5		8	
^{99}Tc (pCi/L)	3.29J	±2.78	15.27	±3.42	3.35J	±2.83	5.07	±2.92
WB3D								
TCE (µg/L)	8.4		21		10		8	
^{99}Tc (pCi/L)	4.98	±2.86	15.33	±3.44	5.02	±2.89	6.74	±2.97
MS1U								
TCE (µg/L)	6.0		27		7.2		12	
^{99}Tc (pCi/L)	1.65J	±2.75	17.04	±3.54	5.06	±2.91	6.82	±3.00
MS1D								
TCE (µg/L)	5.4		28		8.8		16	
^{99}Tc (pCi/L)	1.65J	±2.75	18.67	±3.64	6.82	±3.00	8.42	±3.04
WB1.5 U								
TCE (µg/L)	5.8		28		8.5		14	
^{99}Tc (pCi/L)	4.98	±2.86	16.52	±3.43	5.04	±2.89	3.37J	±2.85
WB1.5D								
TCE (µg/L)	6.2		26		8.6		17	
^{99}Tc (pCi/L)	3.31J	±2.80	16.73	±3.48	3.39J	±2.87	8.54	±3.08
WB1U								
TCE (µg/L)	6.2		26		8.9		12	
^{99}Tc (pCi/L)	3.28J	±2.77	15.15	±3.40	5.08	±2.92	6.77	±2.98
WB1D								
TCE (µg/L)	6.1		25		8.6		13	
^{99}Tc (pCi/L)	3.29J	±2.78	15.27	±3.42	5.10	±2.93	6.73	±2.96
EB2U								
TCE (µg/L)	5.6		24		8.5		15	
^{99}Tc (pCi/L)	3.31J	±2.80	17.03	±3.54	8.46	±3.05	6.80	±3.00
EB2D								
TCE (µg/L)	5.4		22		8.2		14	
^{99}Tc (pCi/L)	4.95	±2.85[a]	11.81	±3.21[a]	5.94	±2.96[a]	5.96	±2.97[a]

Blank = no data; ± = ^{99}Tc counting error; J = value less than laboratory reporting limit; < = BDL value.
[a]Average of duplicate analyses on a single sample or on split samples.

reflect downwelling of stream water within the bed (Harvey and Wagner 2000). Increases in Q_g may include a component of upwelling stream water or runoff, although the lack of precipitation in the 24 h preceding each gauging run suggests that runoff was minimal. Error in Q_{dye} measurements, which Clow and Fleming (2008) reported as 7% to 11%, is related in part to the assumption of 1-D flow along the stream. We injected dye across a relatively straight, narrow, shallow reach. During gauging, stream width along the reach was 2.57 to 7.95 m and stream depth was ≤0.44 m. Mixing lengths, which were calculated for each round of dye injection following Kilpatrick and Cobb (1985), ranged from 9 m (January 2011) to 40 m (February 2012) (Tripathi 2013). The initial sampling location (WB3U) was approximately 40 m downstream of the dye-injection site, which suggests relatively complete mixing. However, observations of RWT retention in stagnant zones along the banks and small, secondary RWT peaks at WB3U (Tripathi 2013) indicate incomplete transverse mixing, as noted by Mukherjee et al. (2005) for a 241-m reach downstream of EB2D. Given the relatively short duration of each dye trace (<4 h), sorption and photodegradation of RWT should have had a minimal effect on Q_{dye} values (Runkel 2015). Measured increases in discharge for the entire reach were broadly similar: values of ΔQ_{dye} were 75.5% to 139% of ΔQ_g, and the differences

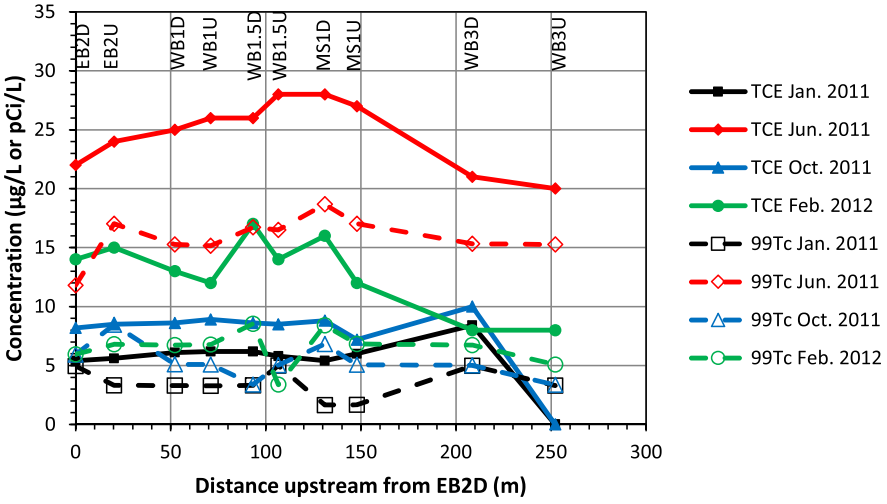

Figure 6. TCE and ^{99}Tc concentrations in stream water as a function of distance along Little Bayou Creek for January 2011, June 2011, October 2011, and February 2012. Unquantified BDL values plotted as 0.

between ΔQ_{dye} and ΔQ_g in June and October 2011 (1.1% to 7.0%) were < 1 L/s.

Median q_{net} values from gauging and dye dilution exceeded maximum q_z values from temperature probing and were approximately two orders of magnitude greater than median q_z values. The q_{net} values represent stream-surface areas of 82.1 to 692 m^2, whereas each q_z value represents a gridded area of approximately 2.8 m^2. Consequently, q_{net} should average out smaller-scale variations in groundwater discharge. If all discharge is focused through areas of the streambed with thermal anomalies, the discrepancy between q_{net} and q_z values is even greater. Mapped $T(z)$ values of 13 to 17 °C represented only approximately 3% of the study reach in January 2011 and approximately 6% of the study reach in August 2011. Sources of uncertainty in q_z include the assumed value of K_{fs}, which should vary by a factor of approximately 3 (0.8 to 2.5 J/(s-m-K); Schmidt et al. 2007), and, more fundamentally, the assumption of steady-state 1-D flow. The range of probing depths in this study was broader than the 0.2 to 0.5 m recommended by Schmidt et al. (2007). At z < 0.2 m, diurnal temperature oscillations can be significant, and at z > 0.5 m (or where piping occurs), streambed and groundwater temperatures converge, thus causing nonsensical solutions to Equation (3). In addition, q_z values underestimate actual fluxes if discharge in the streambed is subvertical (Schmidt et al. 2007).

Temporal Variability in Flow, Contaminant Concentrations, and Fluxes

The farthest downstream (EB2D) and upstream (WB3U) gauging sites in this study correspond to sites LBC-4 and LBC-5, respectively, of LaSage et al. (2008a, 2008b). Those authors monitored flow and water quality along the study reach at quarterly (2 to 4 month) intervals from September 1999 through May 2001. Ranges of Q_g at EB2D and WB3U overlapped those in LaSage et al. (2008b), who reported minimum Q_g values at the same time of year (January 2000) as in this study and maximum values in June 2000. Likewise, our range of ΔQ_g values (9.1-44.2 L/s) overlapped that of LaSage et al. (2008b) (5.20-18.7 L/s). Ranges of Q_{spr} were similar (0.0064-2.14 L/s for 2011-2012; 0.003-2.8 L/s for 1999-2001), with the maximum occurring at WB3 in both studies. In both studies, Q_{spr} values tended to be lowest in January. LaSage et al. (2008b) attributed seasonal variations in stream and spring discharge, which broadly tracked hydraulic-head fluctuations in a near-stream monitoring well, to seasonal variability in recharge.

Temperature probing occurred along the study reach at similar grid spacing in August 2002 (LaSage et al. 2008b) as in January and August 2011. In general, thermal anomalies were spatially persistent over 9 years, although some discharge locations migrated several meters (Figure 4). Spring WB3 emerged between January and May 2000 (LaSage et al. 2008b) and persisted at approximately the same location, although the orifice evolved as a result of piping and stream erosion. Besides WB1, WB2, and WB3, other springs observed by LaSage et al. (2008b) that persisted throughout this study included EB2, EB3, and EB4, although discharge from EB4 decreased to the extent that it could not be measured. Springs observed by LaSage et al. (2008b) that were not visible in this study included EB1 (along the east bank near site EB2D), MS2, and RR (along the tributary RRS upstream of WB3U). The thermal anomaly along reach 1 at approximately 190 m may have coincided with the new location of MS2, which was located at approximately 180 to 200 m in 2002. Similarly, MS1 appears to have evolved into orifices along the east bank (MS1E) and west bank (MS1W) between 2002 and 2010. Springs that emerged during this study included WB0.5, WB1.1, EB5, MS1EU, and an unnamed streambed spring at 125 to 130 m along reach 2, where August 2011 temperature probing indicated a weak anomaly. Zones with $T(z) \leq 17$ °C represented approximately 6% of the total area of the study reach in August 2011, while zones with $T(z)$ < 16.5 °C represented approximately 7.5% of the area in August 2002 (LaSage et al. 2008b). For springs with at least 4 quarters' worth of data, temperatures

Table 3

TCE and ^{99}Tc Concentrations in Springs

	January 2011		June 2011		October 2011		February 2012	
WB3								
TCE (µg/L)	160		100		110		100	
^{99}Tc (pCi/L)	51.68	±6.24	37.50	±4.94	38.00	±5.00	34.10	±4.64
WB2								
TCE (µg/L)	59		64		59		65	
^{99}Tc (pCi/L)	27.45	±4.16	24.46	±3.96	24.17	±3.82	39.24	±5.09
MS1EU								
TCE (µg/L)					70		141	
^{99}Tc (pCi/L)					27.88	±4.15	50.60	±6.10
MS1E								
TCE (µg/L)			<5		<5		10	
^{99}Tc (pCi/L)			<4.68	±2.74	5.76	±2.74[a]	6.47	±2.73
MS1W								
TCE (µg/L)	17		30		24		38	
^{99}Tc (pCi/L)	7.98	±2.88	14.69	±3.29	11.48	±3.12	20.78	±3.56
EB5								
TCE (µg/L)	<5		<5		<5		3J	
^{99}Tc (pCi/L)	1.61J	±2.67	<4.61	±2.70	3.26J	±2.76	1.63J	±2.71
EB4								
TCE (µg/L)					<5			
^{99}Tc (pCi/L)					1.61J	±2.67		
WB1.1								
TCE (µg/L)							4J	
^{99}Tc (pCi/L)							<4.52	±2.62
WB1								
TCE (µg/L)	6.5		5		5.5		5	
^{99}Tc (pCi/L)	3.20J	±2.70	3.26J	±2.75	1.65J	±2.74	1.62J	±2.69
EB3								
TCE (µg/L)			<5				4J	
^{99}Tc (pCi/L)			1.61J	±2.68			<4.67	±2.74
WB0.5								
TCE (µg/L)			<5					
EB2								
TCE (µg/L)	<5		<5		<5		<5	
^{99}Tc (pCi/L)	<4.33	±2.54	<4.51	±2.62	1.60J	±2.67	<4.53	±2.65

Blank = no data; ± = ^{99}Tc counting error; J = value less than laboratory reporting limit; < = BDL value.
[a]Average of duplicate analyses on a single sample or on split samples.

were similar in each study (medians of 13.6-14.2 °C for 2011-2012; means of 13.9-14.6 °C for 1999-2001).

In general, contaminant concentrations in stream water and springs decreased from 1999 to 2001 to 2011 to 2012. In both studies, contaminant concentrations in stream water increased between WB3U and EB2D, with minimum values in January and maximum values in June at each location. At WB3U, the maximum TCE concentration was greater for 2011 to 2012 than for 1999 to 2001 (20 µg/L vs. BDL), whereas the maximum ^{99}Tc concentration was greater for 1999 to 2001 (37.9 vs. 15.27 pCi/L). At EB2D, TCE concentrations were 5.4-22 µg/L for 2011 to 2012 and 7.5-63 µg/L for 1999 to 2001, while ^{99}Tc concentrations were 4.95-11.81 pCi/L for 2011 to 2012 and 14.5-86.7 pCi/L for 1999 to 2001. In this study, maximum concentrations were 160 µg/L for TCE at WB3 in January 2011 and 72.74 pCi/L for ^{99}Tc at RRS in October 2011, versus 450 µg/L for TCE and 461 pCi/L for ^{99}Tc previously (both at MS2 in May 2001). Contaminants were detected in all springs monitored during 1999 to 2001, whereas concentrations in springs downstream of MS1W were usually at or below the detection limit of 5 µg/L for TCE, and were close to or within uncertainty for ^{99}Tc, during 2011 to 2012. In addition, ^{99}Tc

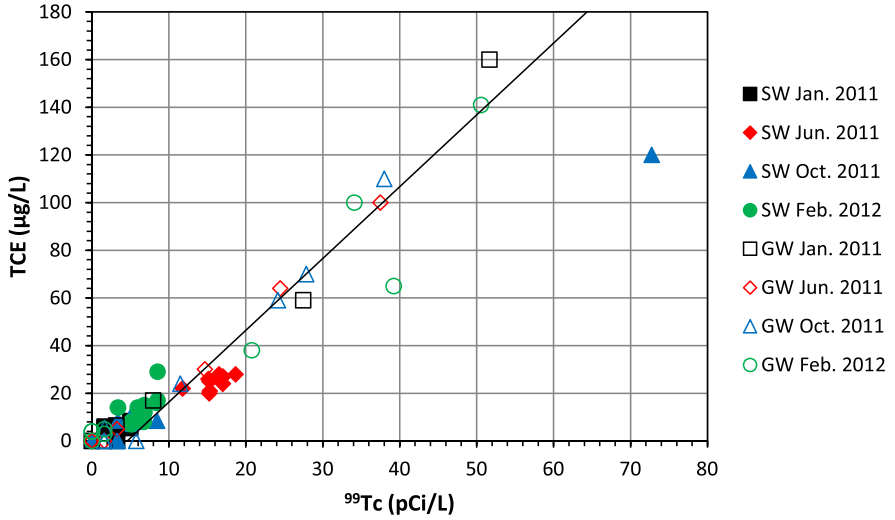

Figure 7. TCE versus ^{99}Tc concentrations in stream water (SW) and springs (GW) for all sampling rounds. Unquantified BDL values plotted as 0. Line represents regression for GW samples with both ^{99}Tc and TCE values above detection limit (TCE = 3.0^{99}Tc – 14; r^2 = 0.91).

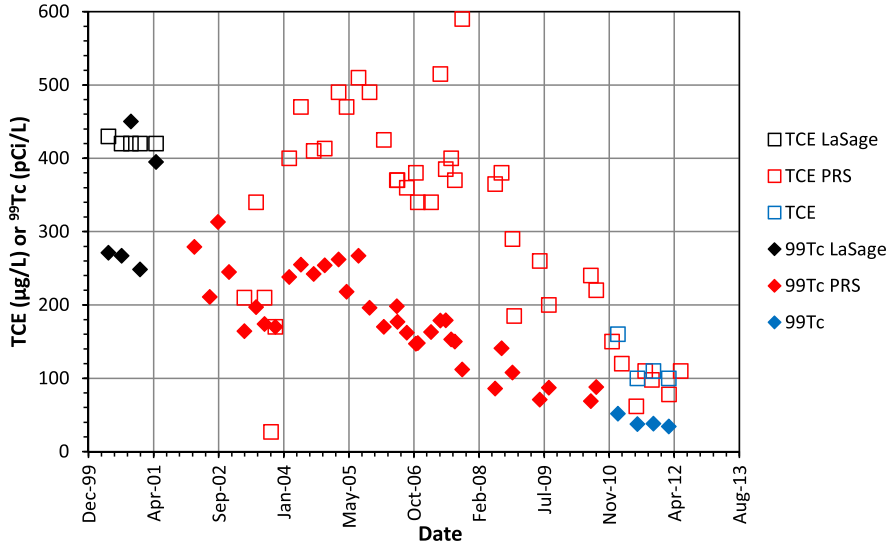

Figure 8. Time series of TCE and ^{99}Tc concentrations in spring WB3 (data from LaSage et al. (2008a), Paducah Remediation Services [PRS] LLC [unpublished], and this study). Replicate values were averaged.

concentrations decreased more than TCE concentrations did. The linear regression between the analytes in springs was TCE = 1.1^{99}Tc + 8.9 (r^2 = 0.86) for 1999 to 2001 (LaSage et al. 2008a) and, considering samples where both analytes were above detection limit, TCE = 3.0^{99}Tc – 14 (r^2 = 0.91) for 2011 to 2012 (Figure 7).

Results of quarterly to semiannual monitoring of WB3 by PGDP contractors (who referred to the spring as LBCSP5) bridge the temporal data gap between LaSage et al. (2008b) and this study. The contractors monitored ^{99}Tc from 2002 to 2010 and TCE from 2002 to 2012. Because samples were not collected simultaneously by us and by contractors or analyzed in the same laboratories, exact comparisons are limited. However, a plot of the combined data sets versus time shows that contaminant concentrations gradually decreased, albeit with fluctuations (Figure 8). Dissolved oxygen results for springs in this study (2.60-4.50 mg/L, with values 2.9-4.2 mg/L for 24 of 27 samples) are similar to those of LaSage et al. (2008a) (2.92-5.10 mg/L, with values 3.3-4.5 mg/L for 45 of 47 samples). As observed by LaSage et al. (2008a), other VOCs, including putative daughter products of anaerobic degradation of TCE (less-chlorinated ethenes, such as dichloroethenes and vinyl chloride), were largely undetectable in this study. The only exception was cis-1,2-dichloroethene, which occurred at 5.3 µg/L in RRS in October 2011. Therefore, the decrease in TCE concentrations between 2001 and 2011 is probably not a result of intrinsic reductive dechlorination, which is a common mechanism of TCE attenuation at other sites (LaSage et al. 2008a; Weatherill et al. 2014, 2018). Instead, the decrease in both ^{99}Tc and TCE concentrations is likely attributable to the extraction wells in the northwest plume between PGDP and

Little Bayou Creek. Two wells each in two wellfields were initially installed in August 1995 (Jolly 1996), but portions of the plume beyond the capture zones of the wells continued to discharge to the creek thereafter.

Comparison of estimated contaminant fluxes from extraction wells, springs, and streamflow along the study reach provides insights about the extent of mass removal by remediation versus natural processes between 1999 and 2012. Assuming each of the two downgradient wells (EW-228 and EW-229) pumped 20% of the total reported extraction volume for the month (U.S. Department of Energy 2007), the combined TCE flux from those wells was approximately 3100 µg/s in May 2000 and approximately 10,000 µg/s in December 2000, while the combined ^{99}Tc flux from May 2000 to April 2001 was approximately 1100 to 1500 pCi/s (unpublished data, Paducah Remediation Services LLC). From October 2009 to July 2010 (the last date for which data were available), the combined TCE flux was approximately 24 to 37 µg/s and the combined ^{99}Tc flux was approximately BDL-82 pCi/s for the two downgradient wells. Values of F_r calculated from gauging along the study reach during 1999 to 2001 were 94 to 1460 µg/s for TCE and 182 to 1910 pCi/s for ^{99}Tc, whereas those values were 150 to 860 µg/s and 77 to 310 pCi/s during 2011 to 2012. LaSage et al. (2008a) noted that F_r values varied with seasonal fluctuations in stream flow and groundwater discharge. Springs WB2 and WB3 together represented 55% to 95% of total measured F_{spr} for TCE and 54% to 94% of total measured F_{spr} for ^{99}Tc during 1999 to 2001, while WB3 itself represented 93% to 98% of total measured F_{spr} for TCE and 89% to 96% of total measured F_{spr} for ^{99}Tc during 2011 to 2012. It is evident that the pump-and-treat system reduced but did not eliminate contaminant discharge to Little Bayou Creek, especially along the upper part of the study reach and the upstream tributary RRS.

The continued persistence and evolution of springs along Little Bayou Creek are uncertain because groundwater discharge is likely to decrease. The shut-down of uranium enrichment at PGDP in 2013 reduced daily water usage by a factor of approximately 10 (Paducah-Portsmouth Project Office 2020). During 2006, the facility used an average of 4.96×10^7 L/d of water (PGDP Groundwater Modeling Working Group 2008), which was piped from the Ohio River. Assuming a leakage rate like that of municipal distribution systems (19%; Jowitt and Xu 1990), the PGDP Groundwater Modeling Working Group (2008) estimated an anthropogenic recharge rate as high as 1.2 m/year, versus meteoric recharge estimates of 0.0671 to 0.194 m/year. In addition, Ohio River pool elevation increased from 88.4 m to 92.0 m asl in 2018 with completion of Olmsted Lock and Dam approximately 27 km downstream of the mouth of Bayou Creek (U.S. Army Corps of Engineers 2018). Assuming an average h of 100 m asl in the RGA beneath PGDP (Fryar et al. 2000), which could fall with reduced recharge, the lateral hydraulic gradient could decrease by at least 45%.

Summary and Conclusions

Using a combination of techniques at spatial scales of meters to hundreds of meters, we have documented persistence and variability in groundwater and contaminant discharge along a channelized stream in unlithified sediments at seasonal to decadal time scales, building on LaSage et al. (2008a, 2008b). In general, baseflow measured by both gauging and dye dilution increased with distance down the study reach. Both stream and spring discharge varied seasonally, with greatest values in February to June and minimum values in October to January. Spring temperatures clustered around median values of approximately14 °C. Temperature probing on a grid in January and August 2011 identified thermal anomalies that occupied small areas of the streambed (~3% to 6% of the ~300-m-long reach) and typically coincided with visible springs or seeps. Locations of anomalies were similar to those identified by temperature probing in summer 2002, although some springs migrated several meters (i.e., some orifices disappeared and others emerged). Point values of vertical groundwater flux calculated from temperature probing in 2011 tended to be less than subreach-scale net fluxes calculated from stream discharge measurements. We surmise that the difference primarily reflects limitations in the assumption of 1D, steady-state flow on which the point-flux calculations were based. As observed by LaSage et al. (2008a) during 1999 to 2001, TCE and ^{99}Tc concentrations in stream water and springs during 2011 to 2012 tended to be higher along the upstream half of the study reach, and concentrations in springs covaried. However, maximum concentrations and contaminant fluxes decreased between 1999 to 2001 and 2011 to 2012, particularly for ^{99}Tc, which we attribute to partial interception of the northwest plume by pumping wells between PGDP and Little Bayou Creek.

Our findings corroborate the observations of Guhman and Pederson (1992) that springs in unlithified sediments can remain stationary within a few meters over decadal (or longer) time scales. Moreover, seasonal variability in groundwater discharge may be greater than annual or decadal variability for a given season. For example, the twofold increase in the area of temperature anomalies from January to August 2011 was greater than the difference between August 2002 and August 2011, which may reflect the water table being higher in August than in January (LaSage et al. 2008b). However, anthropogenic changes to recharge (through curtailment of industrial operations) and base level (through impoundment of a new pool on the Ohio River) are likely to have pronounced impacts on groundwater flow and discharge along Little Bayou Creek, as channelization did (LaSage et al. 2008b).

Acknowledgments

This work was funded by DOE through the Kentucky Research Consortium for Energy and Environment. However, the contents of the paper do not necessarily reflect the views and policies of DOE. We thank DOE, TVA, and the Kentucky Department of Fish and Wildlife Resources for providing access; Brian Begley (Kentucky Department for Environmental Protection) for providing data; Jim Currens (KGS) for help with dye analyses; and Kelley Lynn, Steve Meiners, Brandon Dailey, Jeremy Paessler, and Ahmed Fekri for assistance with field work. Claudia Varnier and Ty Ferré provided helpful review comments on the paper. Data are available upon request from A.E. Fryar.

Supporting Information

Additional Supporting Information may be found in the online version of this article. Supporting Information is generally not peer reviewed.

Table S1 Net stream fluxes between pairs of gauging and dye monitoring sites.

Table S2. Calculated contaminant fluxes to Little Bayou Creek. Blank values represent instances where F_{spr} was not measured. Unquantified BDL concentrations taken as 0.

References

Almayahi, A., and E.W. Woolery. 2018. Fault-controlled contaminant plume migration: Inferences from SH-wave reflection and electrical resistivity experiments. *Journal of Applied Geophysics* 158: 57–64.

Briggs, M.A., E.B. Voytek, F.D. Day-Lewis, D.O. Rosenberry, and J.W. Lane. 2013. Understanding water column and streambed thermal refugia for endangered mussels in the Delaware River. *Environmental Science & Technology* 47, no. 20: 11423–11431.

Bruegger, K. 2017. World map of the Köppen-Geiger climate classification updated map for the United States of America. Climate Change & Infectious Diseases Group, University of Veterinary Medicine, Vienna. http://koeppen-geiger.vu-wien.ac.at/usa.htm (accessed April 16, 2020).

Clausen, J.L., J.W. Douthitt, K.R. Davis, and B.E. Phillips. 1992. Report of the Paducah Gaseous Diffusion Plant groundwater investigation Phase III. Report KY/E-150, prepared for the U.S. Department of Energy under subcontract to DOE contract DE-AC05-76OR00001. Kevil, Kentucky: Martin Marietta Energy Systems.

Clow, D.W., and A.C. Fleming. 2008. Tracer gauge: An automated dye dilution system for ice-affected streams. *Water Resources Research* 44, no. 12: W12441. https://doi.org/10.1029/2008WR007090

Conant, B. Jr. 2004. Delineating and quantifying ground water discharge zones using streambed temperatures. *Groundwater* 42, no. 2: 243–257.

Davidson, G.R., J.R. Rigby, D. Pennington, and J.V. Cizdziel. 2013. Elemental chemistry of sand-boil discharge using to trace variable pathways of seepage beneath levees during the 2011 Mississippi River flood. *Applied Geochemistry* 28: 62–68.

Evaldi, R.D., and D.L. McClain. 1989. Streamflow, specific-conductance, and temperature data for Bayou and Little Bayou Creeks near Paducah, Kentucky, August 15 and 16, 1989. U.S. Geological Survey Open-File Report 89-582. Louisville, Kentucky: USGS.

Fryar, A.E., E.J. Wallin, and D.L. Brown. 2000. Spatial and temporal variability in seepage between a contaminated aquifer and tributaries to the Ohio River. *Groundwater Monitoring & Remediation* 20, no. 3: 129–146.

Guhman, A.I., and D.T. Pederson. 1992. Boiling sand springs, Dismal River, Nebraska: Agents for formation of vertical cylindrical structures and geomorphic change. *Geology* 20, no. 1: 8–10.

Hagerty, D.J. 1991a. Piping/sapping erosion: I. basic considerations. *Journal of Hydrologic Engineering* 117, no. 8: 991–1008.

Hagerty, D.J. 1991b. Piping/sapping erosion: II. identification-diagnosis. *Journal of Hydrologic Engineering* 117, no. 8: 1009–1025.

Harvey, J.W., and B.J. Wagner. 2000. Quantifying hydrologic interactions between streams and their subsurface hyporheic zones. In *Streams and Ground Waters*, ed. J.B. Jones, and P.J. Mulholland, 3–44. San Diego, California: Academic Press.

Hare, D.K., M.A. Briggs, D.O. Rosenberry, D.F. Boutt, and J.W. Lane. 2015. A comparison of thermal infrared to fiber-optic distributed temperature sensing for evaluation of groundwater discharge to surface water. *Journal of Hydrology* 530: 153–166.

Hyun, Y., H. Kim, S.-S. Lee, and K.-K. Lee. 2011. Characterizing streambed water fluxes using temperature and head data on multiple spatial scales in Munsan stream, South Korea. *Journal of Hydrology* 402: 377–387.

Jolly, D.R. 1996. First annual report for the northwest plume interim remedial action pilot plant at the Paducah Gaseous Diffusion Plant, Paducah, Kentucky. U.S. Department of Energy report DOE/OR/07-1531&D1. Kevil, Kentucky: Environmental Management and Enrichment Facilities.

Jowitt, P.W., and C. Xu. 1990. Optimal value control in water-distribution networks. *Journal of Water Resources Planning and Management* 116: 455–472.

Kikuchi, C.P., T.P.A. Ferré, and J.M. Welker. 2012. Spatially telescoping measurements for improved characterization of ground water–surface water interactions. *Journal of Hydrology* 446-447: 1–12.

Kilpatrick, F.A., and E.D. Cobb. 1985. Measurement of discharge using tracers. U.S. Geological Survey Techniques of Water-Resources Investigations, Book 3, Chapter A16. Washington, D.C.: U.S. Government Printing Office.

Krause, S., T. Bloom, and N.J. Cassidy. 2012. Investigating patterns and controls of groundwater up-welling in a lowland river by combining fibre-optic distributed temperature sensing with observations of vertical hydraulic gradients. *Hydrology and Earth System Sciences* 16, no. 6: 1775–1792.

LaSage, D.M., A.E. Fryar, A. Mukherjee, N.C. Sturchio, and L. Heraty. 2008a. Groundwater-derived contaminant fluxes along a channelized Coastal Plain stream. *Journal of Hydrology* 360: 265–280.

LaSage, D.M., J.L. Sexton, A. Mukherjee, A.E. Fryar, and S.F. Greb. 2008b. Groundwater discharge along a channelized Coastal Plain stream. *Journal of Hydrology* 360: 252–264.

Li, Y., J. Craven, E.S. Schweig, and S.F. Obermeier. 1996. Sand boils induced by the 1993 Mississippi River flood: Could they one day be misinterpreted as earthquake-induced liquefaction? *Geology* 24, no. 2: 171–174.

Lin, A., M. Kikuchi, and B. Fu. 2003. Rupture segmentation and process of the 2001 Mw 7.8 central Kunlun, China, earthquake. *Bulletin of the Seismological Society of America* 93, no. 6: 2477–2492.

Mukherjee, A., A.E. Fryar, and D.M. LaSage. 2005. Using tracer tests to assess natural attenuation of contaminants along a channelized Coastal Plain stream. *Environmental & Engineering Geoscience* 11, no. 4: 371–382.

National Research Council. 2004. *Groundwater Fluxes Across Interfaces*. Washington, D.C.: National Academies Press.

Olive, W.W. 1980. Geologic maps of the Jackson Purchase region, Kentucky. U.S. Geological Survey Miscellaneous Investigations Series Map I-1217. Washington, D.C.: USGS.

Paducah-Portsmouth Project Office. 2020. Paducah GDP shutdown and deactivation. https://www.energy.gov/pppo/paducah-gdp-shutdown-and-deactivation (accessed April 28, 2020).

PGDP Groundwater Modeling Working Group. 2008. 2008 update of the Paducah Gaseous Diffusion Plant sitewide groundwater flow model. Report PRS-ENR-0028, prepared for the U.S. Department of Energy. Kevil, Kentucky: Paducah Remediation Services LLC.

Poulsen, J.R., E. Sebok, C. Duque, D. Tetzlaff, and P.K. Engesgaard. 2015. Detecting groundwater discharge dynamics from point-to-catchment scale in a lowland stream: Combining hydraulic and tracer methods. *Hydrology and Earth System Sciences* 19, no. 4: 1871–1886.

Rantz, S.E. 1982. Measurement and computation of streamflow, volume 1, measurement of stage and discharge. U.S. Geological Survey Water-Supply Paper 2175. Washington, D.C.: U.S. Government Printing Office.

Rosgen, D., and L. Silvey. 1998. *Field Guide for Stream Classification*, 2nd ed. Ft. Collins, Colorado: Wildland Hydrology Books.

Rosenberry, D.O., M.A. Briggs, G. Delin, and D.K. Hare. 2016. Combined use of thermal methods and seepage meters to efficiently locate, quantify, and monitor focused groundwater discharge to a sand-bed stream. *Water Resources Research* 52, no. 6: 4486–4503.

Runkel, R.L. 2015. On the use of rhodamine WT for the characterization of stream hydrodynamics and transient storage. *Water Resources Research* 51, no. 8: 6125–6142.

Schmidt, C., B. Conant Jr., M. Bayer-Raich, and M. Schirmer. 2007. Evaluation and field-scale application of an analytical method to quantify groundwater discharge using mapped streambed temperatures. *Journal of Hydrology* 347: 292–307.

Schmidt, C., M. Bayer-Raich, and M. Schirmer. 2006. Characterization of spatial heterogeneity of groundwater-stream water interactions using multiple depth streambed temperature measurements at the reach scale. *Hydrology and Earth System Sciences* 10, no. 6: 849–859.

Stelzer, R.S., E.A. Strauss, and M. Coulibaly. 2017. Assessing the importance of seepage and springs to nitrate flux in a stream network in the Wisconsin sand plains. *Hydrological Processes* 31, no. 11: 2016–2028.

Tripathi, G.N. 2013. Spatio-temporal variability in groundwater discharge and contaminant fluxes along a channelized stream in western Kentucky. Ph.D. dissertation, University of Kentucky, Lexington, Kentucky, 127 p. https://uknowledge.uky.edu/ees_etds/13/ (accessed April 13, 2020).

Turcotte, D.L., and G. Schubert. 1982. *Geodynamics: Applications of Continuum Physics to Geological Problems*. New York: John Wiley & Sons.

University of Kentucky Agricultural Weather Center. 2020a. Kentucky climate data, Paducah. http://weather.uky.edu/ky/data.php#KY_Climate_Data (accessed April 16, 2020).

University of Kentucky Agricultural Weather Center. 2020b. Kentucky observed climate normals (1981-2010). http://weather.uky.edu/ky/climate.php#Kentucky_Normals (accessed April 16, 2020).

U.S. Army Corps of Engineers. 2018. Louisville District, Olmsted Locks and Dam. https://www.lrl.usace.army.mil/Missions/Civil-Works/Navigation/Locks-and-Dams/Olmsted-Locks-and-Dam/ ().

U.S. Department of Energy. 2007. Groundwater remedial system performance optimization at PGDP, Paducah, Kentucky. Review report prepared for the Office of Environmental Management. Washington, D.C.: U.S. Department of Energy.

Weatherill, J.J., S. Atashgahi, U. Schneidewind, S. Krause, S. Ullah, N. Cassidy, and M.O. Rivett. 2018. Natural attenuation of chlorinated ethenes in hyporheic zones: A review of key biogeochemical processes and in-situ transformation potential. *Water Research* 128: 362–382.

Weatherill, J., S. Krause, K. Voyce, F. Drijfhout, A. Levy, and N. Cassidy. 2014. Nested monitoring approaches to delineate groundwater trichloroethene discharge to a UK lowland stream at multiple spatial scales. *Journal of Contaminant Hydrology* 158: 38–54.

White, D.S., C.H. Elzinga, and S.P. Hendricks. 1987. Temperature patterns within the hyporheic zone of a northern Michigan river. *Journal of the North American Benthological Society* 6, no. 2: 85–91.

Wood, W.W. 1976. Guidelines for collection and field analysis of ground-water samples for selected unstable constituents. U.S. Geological Survey Techniques of Water-Resources Investigations, Book 1, Chapter D2. Washington, D.C.: U.S. Government Printing Office.

Biographical Sketches

***Ganesh N. Tripathi**, senior divisional geologist, Department of Mines and Geology, Ministry of Industry, Commerce and Supplies, Government of Nepal, Lainchour, Kathmandu, Nepal; ganeshtri@gmail.com.*

***Alan E. Fryar**, corresponding author, professor, is at the Department of Earth and Environmental Sciences, University of Kentucky, 101 Slone Building, Lexington, KY 40506-0053; alan.fryar@uky.edu.*

***Steven K. Hampson**, research program manager, is at the Center for Applied Energy Research, University of Kentucky, 2540 Research Park Dr., Lexington, KY 40511; skhampson@windstream.net*

***Abhijit Mukherjee**, associate professor, is at the Department of Geology and Geophysics and School of Environmental Science and Engineering, Indian Institute of Technology Kharagpur, Kharagpur 721302, India; amukh2@gmail.com.*